A one-phase thermomechanical constitutive model for the numerical simulation of semi-solid thixoforming

R. Koeune[1], J.-P. Ponthot[2]

[1]University of Liège - Sart-Tilman, 4000 Liège, Belgium
URL: http://www.ltas-mnl.ulg.ac.be e-mail: r.koeune; JP.Ponthot@ulg.ac.be

ABSTRACT: A thermomechanical one-phase elasto-visco-plastic constitutive law has been developed in order to model thixoforming processes. The simulation of a simple academic 2D test has revealed the forces and weaknesses of the proposed model.

KEYWORDS: Finite Element Method (FEM), Thixoforming, Semi-solid, Thermo-mechanical coupling

1 INTRODUCTION

Semi-solid thixoforming is a forming process at temperatures located inside the fusion interval. It relies on a semi-solid microstructure made of globular solid grains more or less connected to each other, thus forming a solid skeleton deforming into a liquid phase. This particular microstructure makes semi-solid materials behave as solids at rest and as liquids during shearing, which causes a decrease of the viscosity and of the resistance to deformation while shearing.
The goal of this research was a selection of constitutive laws to model such behavior. The presented models have been implemented into the finite element code METAFOR and used to simulate a compression test.

2 PRESENTATION OF THE PROPOSED CONSTITUTIVE LAWS

The constitutive law should be able to simulate the complex rheology of semi-solid materials, under both steady-state and transient conditions. For example, the peak of viscosity at start of a fast loading should be appropriately reproduced. Neither liquid formalism nor rigid models can predict residual stresses. Furthermore, the use of a finite yield stress σ_y is appropriate because a vertical billet does not collapse under its own weight unless the liquid fraction is too high.
The basic idea is then to extend the Norton-Hoff law to solid hypoelastic formulation, considering the elastic part of the deformation and two non-dimensional internal parameters. Thus, the extended consistency equation is written as:

$$\overline{\sigma}^{VM} - \sigma_y - k(\dot{\overline{\epsilon}}^{vp})^m = 0 \tag{1}$$

where $\overline{\sigma}^{VM}$ = equivalent Von Mises stress, k = a viscosity parameter, m = strain rate sensibility, and $\dot{\overline{\epsilon}}^{vp}$ = equivalent plastic strain rate.
By analogy with liquid formalism, the **apparent viscosity** η has been defined as:

$$\eta = k(\dot{\overline{\epsilon}}^{vp})^{(m-1)} \tag{2}$$

2.1 Independent internal parameters

The first internal parameter is the **cohesion degree** λ and is illustrated in figure 1. During the process, the material structure changes with the strain history due to the agglomeration of the particles and the breaking of the grains bonds. So, λ is a structural parameter that characterizes the degree of structural build-up in the microstructure: $\lambda = 1$ if the structure is fully built-up and $\lambda = 0$ if the structure is fully broken.
Then, the evolution of the structural parameter λ is described by the equation:

$$\frac{d\lambda}{dt} = \underbrace{a(1-\lambda)}_{build-up} - \underbrace{b\lambda e^{c\dot{\overline{\epsilon}}^{vp}}(\dot{\overline{\epsilon}}^{vp})^d}_{breakdown} \tag{3}$$

where a, b, c and d = material parameters.
It is assumed that the structure is fully built-up at the start of the forming process ($\lambda_0 = 1$).

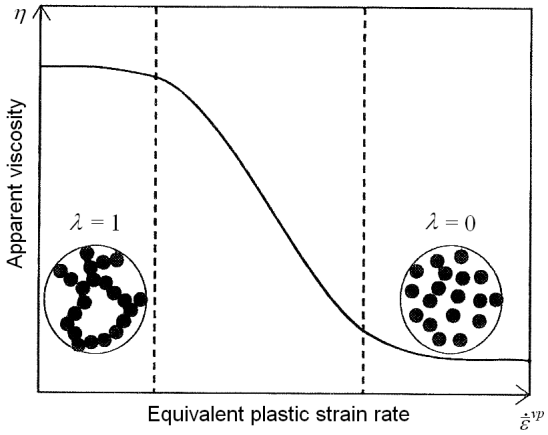

Figure 1: Illustration of the cohesion degree λ

The second internal parameter is the **liquid fraction** f_l. It depends only on the temperature by the Scheil equation [1].

$$f_l = \left(\frac{T - T_s}{T_l - T_s}\right)^{\frac{1}{r-1}} \tag{4}$$

where r = equilibrium partition ratio, T_s and T_l = solidus and liquidus temperatures respectively.

2.2 Correlated internal parameters

In this model, the liquid fraction and the cohesion degree are defined independently, which is not physically based. Actually, the cohesion degree depends on the liquid fraction since it should be unity at solid state, and zero at liquid state. So, in the present state, this model is not extensible to pure solid or liquid behavior.
To overcome this limitation, we can use a cohesion degree that depends on the liquid fraction. By solving the differential equation (3), we can adapt it and introduce the liquid fraction in order to degenerate properly to a pure solid or liquid state behavior. We get:

$$\frac{d\lambda}{dt} = a(1 - f_l)(1 - \lambda) - b f_l \lambda e^{c\dot{\bar{\epsilon}}^{vp}} (\dot{\bar{\epsilon}}^{vp})^d \tag{5}$$

It is still assumed that the structure is fully built-up at the start of the forming process ($\lambda_0 = 1$).

2.3 Viscosity law

Internal parameters interfere in the constitutive law via both viscosity and isotropic hardening laws. The cohesion degree mainly influences the viscosity law, while the main internal parameter in the isotropic hardening law is the liquid fraction.
The viscosity increases with the cohesion degree, but decreases with melting. Both internal parameters are introduced in the viscosity law via the parameters k and m, according to:

$$\begin{aligned} k &= k_1 e^{k_2(1-f_l)}\, e^{k_3\lambda} \\ m &= (m_3\lambda^2 + m_4\lambda + m_1)\, e^{m_2(1-f_l)} \end{aligned} \tag{6}$$

where k_1, k_2, k_3, m_1, m_2, m_3 and m_4 = material parameters.

2.4 Yield and isotropic hardening law

An extended Shima and Oyane [2] isotropic hardening law has been developed. As a liquid does not display yield, this law takes into account a decrease of the yield stress with temperature elevation. A term of linear hardening has been added to initial Shima and Oyane law in order to meet a classical linear hardening law at solid state $f_l = 0$.
G.R. Burgos [3] identified an empirical law that describes the variation of the yield stress with the cohesion degree. The global proposed hardening law is expressed by:

$$\begin{aligned} \sigma_y &= f(\lambda)(\sigma_y^0 + h_1\, \bar{\epsilon}^{vp})\, (1 - f_l)^{h_2} \\ f(\lambda) &= y_a \left[\arctan \frac{y_b y_c}{y_d} + \arctan\left(y_b \frac{\lambda - y_c}{y_d - \lambda}\right)\right] \end{aligned} \tag{7}$$

where h_1, h_2, y_a, y_b, y_c and y_d = material parameters.

3 APPLICATION OF THE PROPOSED LAWS ON THE SIMULATION OF AN ACADEMIC TEST

As a first validation of the proposed material model, a simple compression test of a cylinder made of Sn-15%wt Pb alloy, described in figure 2, has been simulated and compared to available results on compression load (Kang and Yoon [4]). The material parameters have been found in the literature [3, 4]. The friction coefficient is 0.3 and the initial temperature is such as the initial liquid fraction will be 37%.

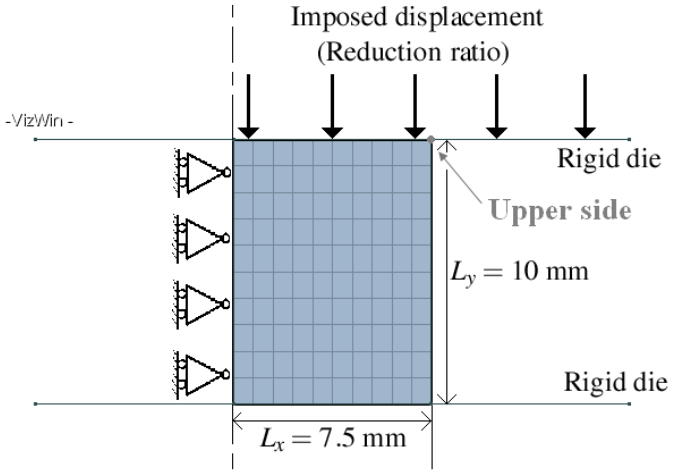

Figure 2: Illustration of the compression test

3.1 Study of the relevance of the material parameters

All material parameters appearing in the proposed model have been reliably determined for Sn-15%wt Pb alloy. But this induce a tremendous amount of experiments that may not be applied on higher melting point alloys such as steel. So, the relevance of some material parameters has been studied in order to reduce the set of parameters. Because of the use a power law, the parameters k_2 and m_2 must remain small, otherwise the viscosity law would be governed by the liquid fraction. The empirical formula of yield stress in terms of the cohesion degree (7) gives interesting results. As shown in figure 3, it predicts an important softening behavior behind a certain level of deformation, which is observed experimentally. But, it causes an excessively high CPU time, and it needs too many material parameters that can not be easily determined. Another possibility is the use of the *effective liquid fraction* f_l^{eff} instead of the liquid fraction in the hardening law. The effective liquid fraction excludes the liquid that is entrapped inside the solid grains and that does not contribute to the flow. With the breaking of the solid bounds some of this entrapped liquid is released, so f_l^{eff} is expressed in terms of the cohesion degree as:

$$f_l^{eff} = f_l(1 - \lambda) \tag{8}$$

This formulation which does not imply the identification of any new material parameter is still under progress. Further simulations presented in this paper use a hardening law that does not depend on the cohesion degree:

$$\sigma_y = (\sigma_y^0 + h_1\, \bar{\epsilon}^{vp})\, (1 - f_l)^{h_2} \tag{9}$$

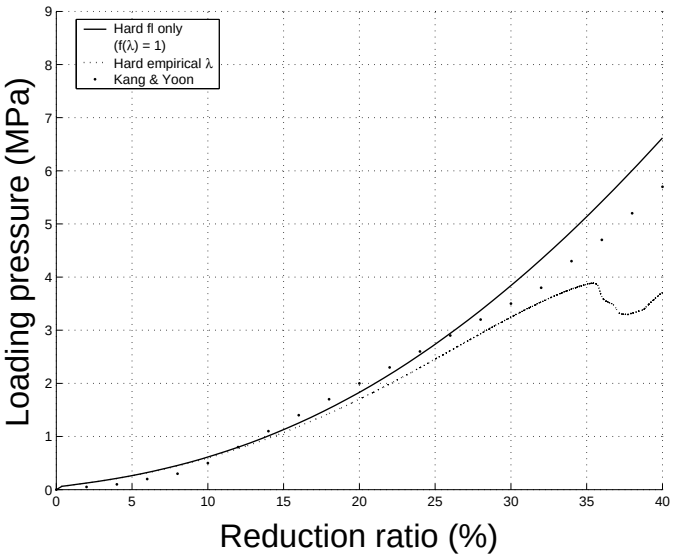

Figure 3: Loading pressure for different hardening laws

3.2 Numerical illustrations

In a first step, the residual stresses have been computed using a quasi-static mechanical analysis with imposed temperature evolution. During the process, the predicted evolution of the loading pressure is in good agreement with the reference [4] (figure 3). After unloading and cooling down, the calculation predicted equivalent Von Mises stresses of 1MPa inside the billet, and a maximum of 800MPa on the surface (not represented).

In figure 4, the results at the upper side of the cylinder of both proposed formulations of the cohesion degree are compared. During the forming process, the drop of temperature due to the contact with the colder die causes a decrease of the liquid fraction. Thus, the formulation (5), which takes the liquid fraction into account, predicts a higher cohesion degree, meaning a higher ratio of solid bounds, than the other one. During the stage of unloading and cooling down to room temperature, the formulation (3), which does not depend on the temperature, predicts a slow recovery of the semi-solid material, while the other cohesion degree tends to one (fully built-up structure) as soon as the solidus is reached, which makes physical sense.

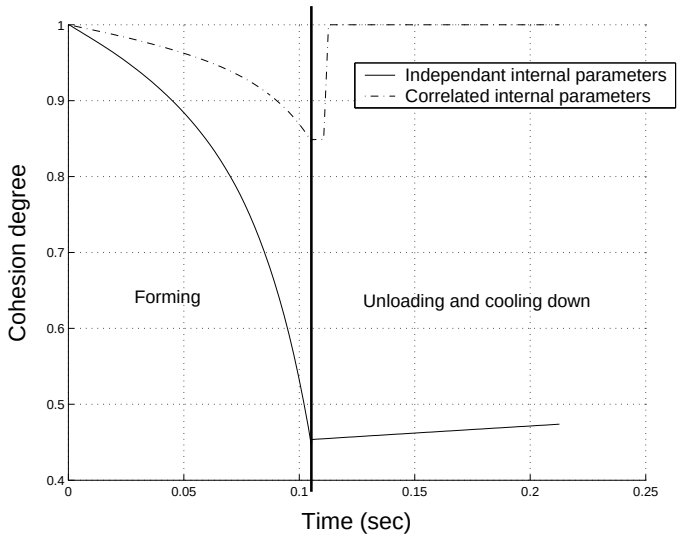

Figure 4: Comparison of both proposed formulations of λ

During a second step, quasi-static thermomechanical simulations have been conducted. In figure 5, the loading pressures for different die temperatures are compared to the reference [4] that results from an isothermal simulation. A decrease of the load with a hotter die can be noted, which confirms the relevance of appropriate die pre-heating.

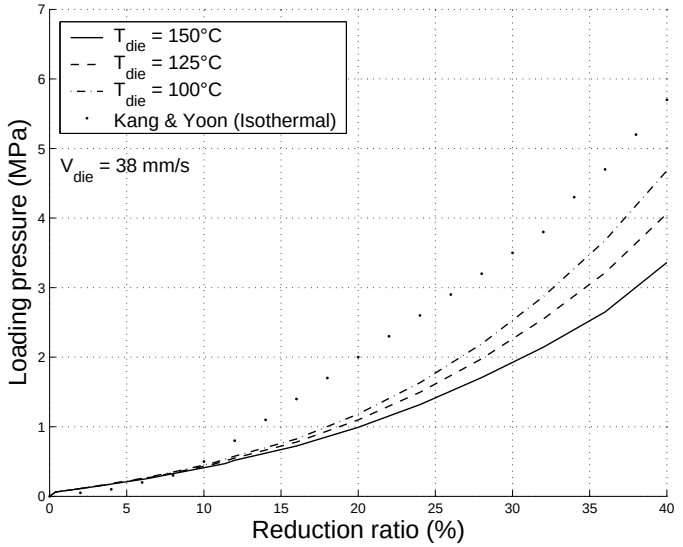

Figure 5: Influence of die temperature on the loading pressure

Finally, the influence of die velocity has been studied using a dynamic mechanical analysis with a uniform imposed drop of temperature of 15°C. In figure 6, the effect of die speed on the apparent viscosity at the upper side of the cylinder is presented. The model can predict the drop of viscosity with shearing, as well as the peak of viscosity at the start of the loading. At high velocities, the apparent viscosity raises significantly if a certain level of deformation is reached. This non physical behavior is due to the fact that the cohesion degree is too low to act sufficiently on the apparent viscosity. In other words, in the present state, the model can not handle free solid grains ($\lambda = 0$) and an enhanced viscosity law needs to be developed.

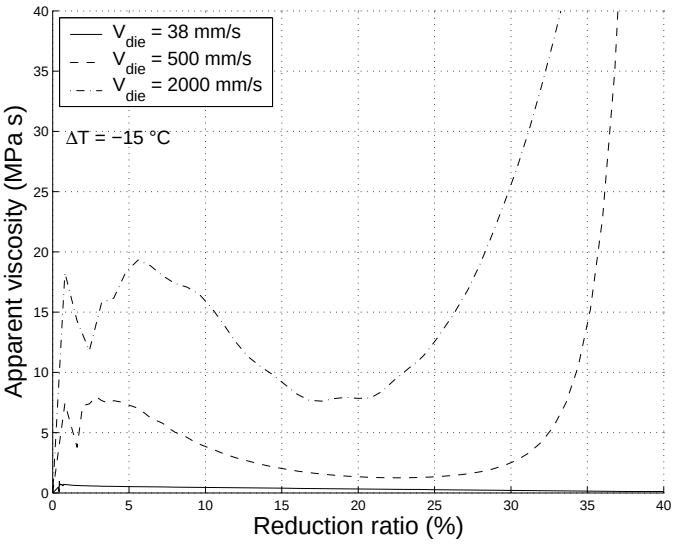

Figure 6: Influence of die speed on the apparent viscosity

4 CONCLUSIONS

Residual stresses, but also thermomechanical and transient behavior occurring in a thixoforming process have been modelled. The proposed model showed good agreement with Kang and Yoon's isothermal simulations, but needs to be accurately validated by comparison of other simulations to experimental data.

REFERENCES

[1] O. Lashkari, and R. Ghomashchi. The implication of rheology in semi-solid metal processes: An overview. *J. of Materials Processing Technology*, 182: 229–240, 2007.

[2] S. Shima, and M. Oyane. Plasticity theory for porous metals. *Int. J. of Mech. Sciences*, 18: 285–291, 1976.

[3] G.R. Burgos, A.N. Alexandrou, and V.M. Entov. Thixotropic rheology of semisolid metal suspensions. *J. of Materials Processing Technology*, 110: 164–176, 2001.

[4] C.G. Kang, and J.H. Yoon. A finite-element analysis on the upsetting process of semi-solid aluminum material. *J. of Materials Processing Technology*, 66: 76–84, 1997.